KSME

Springer

Journal of Mechanical Science and Technology 37 (5) 2023

Original Article
DOI 10.1007/s12206-023-0414-9

Keywords:
· Aerodynamic optimization
· Genetic algorithm
· NACA four-digit airfoils
· Sequential quadratic programming
· Xfoil

Correspondence to:
Durmuş Sinan Körpe
dsinan.korpe@hku.edu.tr

Citation:
Körpe, D. S., Güzelbey, I. H. (2023). NACA four-digit airfoil series optimization: a comparison between genetic algorithm and sequential quadratic programming. Journal of Mechanical Science and Technology 37 (5) (2023) 2375~2382. http://doi.org/10.1007/s12206-023-0414-9

Received July 19th, 2022
Revised December 5th, 2022
Accepted January 15th, 2023

† Recommended by Editor
Han Seo Ko

NACA four-digit airfoil series optimization: a comparison between genetic algorithm and sequential quadratic programming

Durmuş Sinan Körpe and Ibrahim Halil Güzelbey

Department of Aerospace Engineering, Hasan Kalyoncu University, Gaziantep 27010, Türkiye

Abstract In this study, the results of genetic algorithm and sequential quadratic programming are discussed for NACA four-digit airfoil series optimization. The lift-to-drag ratio is defined as the objective function. The aerodynamic constraints related to the lift, drag, moment values of the airfoil at high and low angle of attack, and the geometric constraints related to the wetted length and internal volume are set. Results show that the sequential use of the former and latter methods and the stand-alone use of the latter method yield an increment of approximately 20 % in the objective function. The change in the geometric design variables reveals that the optimum airfoils are obtained by the variation in the maximum camber and thickness. Sequential quadratic programming is proven to converge to the global optimum in a significantly shorter solution time than genetic algorithm when the practical constraints are defined into the optimization problems.

1. Introduction

Airfoils play a key role in aircraft design. Their behavior at different flight speeds and angle of attack values characterizes the aircraft performance. At the early development of airfoil shapes, the national advisory committee by aeronautics (NACA) conducted many wind tunnel tests for NACA four-digit airfoils [1, 2]. Many fixed wing aircrafts were designed using the results obtained in these tests [3].

Nowadays, the aerodynamic optimization of the airfoils has become an attractive research area for fixed and rotary wings due to rapid advances in computer technology. The development of aerodynamic solvers and the use of parallel computing provide the solution of the aerodynamic optimization problems subject to multidisciplinary inequality or equality constraints $(g(x))$ [4, 5].

In general, high-fidelity solvers are not preferred in the preliminary aerodynamic shape optimization studies due to their high computational cost [6]. The most preferred low-fidelity solver is Xfoil [7, 8]. Xfoil, which was developed by Mark Drela, is a Fortran-based software for the aerodynamic analysis of subsonic flow over airfoils. The panel method is integrated into the integral momentum and kinetic energy shape parameter equations, and e^n method is used for the transition prediction. Karman-Tsien method is used for compressibility correction [9].

Herbert-Acero et al. compared 13 different fluid flow models including Xfoil by predicting the lift coefficient (C_l) and the drag coefficient (C_d) of NACA 4412 [10]. The results showed that the predictions of Xfoil and the transition SST model agreed well with the experimental C_d data but Xfoil overpredicted C_l.

Xfoil was used as the function evaluator in many optimization problems related to the fixed wing aircraft [11, 12], the rotary wing aircraft and the propeller [13, 14], and the wind turbines [15, 16].

In this study, the results of aerodynamic optimization problems of NACA four-digit series, which are obtained using the optimization solvers, are discussed. The optimization solvers are genetic algorithm (GA) and sequential quadratic programming (SQP). The lift-to-drag ratio

(C_l/C_d) maximization is defined as the objection function. The maximum camber (m), the location of the maximum camber (p), the maximum thickness (t) of the airfoil, and α values are the design variables. The desired C_l, C_d, and moment coefficient at the quarter-chord (C_m) of the airfoil at high and low α values are defined as the functional constraints. The main contribution of the study to the literature is the addition of these functional constraints to the optimization problem such that the optimization process generates more practical airfoils. The other significant contribution is related to the use of the geometrical constraints. The cross-sectional area (A) and maximum t are the mostly defined geometric constraint in the Refs. [17-19]. In addition to them, wetted length (wl) is defined as a geometric constraint to the optimization problem.

The rest of the paper is organized as follows. In Sec. 2.1, shape generation of NACA four-digit airfoil series is explained. Sec. 2.2 describes the efficient use of Xfoil in optimization problems as the function evaluator. The C_l, C_d, and C_m of NACA 4412, which is the initial airfoil in the optimization problem, at different α values are interpreted for the selection the constraints in Sec. 2.3. Mathematical definition of the optimization problem is described in Sec. 2.4. In Sec. 2.5, the optimization solvers are discussed. Sec. 2.6 presents the results of the optimization problem. Sec. 3 gives the conclusion.

2. Method

2.1 Generation of NACA four-digit airfoil series

In this part, the generation of the half thickness distribution (z_t), the camber distribution (z_c), and their use for shape generation of NACA four-digit airfoil series are discussed [2]. The cosine distribution is used to generate x coordinates. Given that it is coded in Xfoil, NACA airfoil generation subroutine, z_t and z_c values are summed for the z coordinates of the upper surface. The former is subtracted from the later for the z coordinates of the lower surface [20].

According to the NACA four-digit airfoil numbering system, the first digit indicates m in percentage of the chord. The second integer describes the location of p from the leading edge in tenths of the chord. Division of the last two digits to hundred gives t. For example, m, p, and t for NACA 4412 are 0.04, 0.4, and 0.12 for the airfoil that has a unit chord length, respectively. The z_t and z_c of NACA four-digit airfoils are generated using the equations below.

$$z_t(x) = \frac{t}{0.2}\left(0.2969x^{0.5} - 0.126x - 0.3516x^2 + 0.2843x^3 - 0.1036x^4\right) \quad (1)$$

$$z_c(x) = \frac{m}{p^2}\left(2px - x^2\right) \text{ if } 0 \le x < p$$
$$z_c(x) = \frac{m}{(1-p)^2}\left(1 - 2p + 2px - x^2\right) \text{ if } p \le x \le 1 \quad (2)$$

2.2 Xfoil as function evaluator

As discussed above, Xfoil is used in the optimization problems as the function evaluator. In this part, the details of its use are discussed. An interface is adjusted for MAC OS operation system [21] to run Xfoil in MATLAB. The amplification factor (n) of e^n method is selected as 9. The number of panels (N) is selected as 220. Two modifications are implemented into the interface to prevent convergence failure. The first implementation is related to N. When Xfoil fails to converge, N is altered between 216 and 224. The second modification is related to the boundary layer initialization. If the converged solution cannot be obtained for α, then the numerical simulation from α-5 to α-1 is performed for positive α. Then, Xfoil is run for α. The main aim of this process is to start from the converged solution of former α that helps obtain a converged solution for current α. For negative α, the numerical simulation from α+5 to α+1 is performed.

2.3 Aerodynamic characteristics of NACA 4412

In this part, C_l, C_d, and C_m data of NACA 4412 for different α values are discussed. The functional constraints are defined using these data. These α values are selected by considering the level flight performance of an aircraft. The aircraft performs take-off and landing missions at high α around 0.08 Mach (M). At this phase of the flight, $C_{l\max}$ has a key role on the performance. Flight at $C_l/C_{d\max}$ configuration is performed around 0.2 M with a moderate α. The maximum velocity is taken as 0.35 M, and α is low, which is most probably negative, at this phase.

For the analysis, the density (ρ_∞), the speed of sound (a), and the dynamic viscosity (μ_∞) are 1.225 kg/m^3, 340.3 m/s and $1.7974\cdot10^{-5}$ Ns/m^2, respectively. The reference length (c) is 1.5 m. Table 1 shows the free stream velocity (V_∞) and Reynolds number (Re) for the selected M.

By using Xfoil, $C_l-\alpha$, $C_d-\alpha$, $C_l/C_d-\alpha$, and $C_m-\alpha$ results are obtained for the described M values. The significant aerodynamic results for the definition of the functional constraints are summarized in Table 2.

The constraints of the optimization problem in this study are selected by interpreting these data. The objective function $(f(x))$ and $g(x)$ are selected based on the following scenario:

1) The aim of the optimization problem is to maximize C_l/C_d at M = 0.2;

2) The optimum airfoil should provide $C_{l\max}$ of NACA 4412

Table 1. V_∞ and Re for the selected M.

M	V_∞	Re
0.08	27.22	$2.8\cdot10^6$
0.2	68.06	$7\cdot10^6$
0.35	119.11	$1.22\cdot10^7$

Table 2. Significant aerodynamic results of NACA 4412.

M	α(°)	Parameter	Value
0.08	18	$C_{l_{max}}$	1.769
		C_d at $C_{l_{max}}$	0.054
		C_m at $C_{l_{max}}$	−0.0369
0.2	7	$C_l / C_{d_{max}}$	173.56
		C_l at $C_l / C_{d_{max}}$	0.916
		C_m at $C_l / C_{d_{max}}$	−0.0991
0.35	−2	C_l	0.261
		C_d	0.0054
		C_m	−0.1093

at M = 0.08;

3) The C_d of the optimum airfoil can be 10 % greater than the C_d of NACA 4412 at M = 0.08;

4) The C_l of the optimum airfoil at C_l / C_{dmax} case can be 10 % greater or 10 % less than the C_l of NACA 4412 at C_l / C_{dmax} case;

5) The C_d of the optimum airfoil at M = 0.35 should not be greater than the C_d of NACA 4412 at M = 0.35;

6) The C_l of the optimum airfoil at M = 0.35 can be 10 % greater or 10 % less than the C_l of NACA 4412 at M = 0.35,

7) For all flight phases, the C_m of the optimum airfoil can be 75 % greater or 75 % less than the C_m of NACA 4412;

8) wl and A for NACA 4412, which has a c of 1.5 m, are 3.07 m and 0.184 m^2, respectively. In the optimization problem, the maximum increment of 10 % for wl, which is related to the empty weight, is allowed. The maximum decrement of 10 % for A is allowed considering the internal volume requirement of the wing.

Three groups of constraints are observed in the scenario. In the first group, the aerodynamic performance characteristic of NACA 4412 is strictly demanded. The second and fifth articles of the scenario are in this group. The third, fourth, sixth, and eight articles of the scenario that allow a 20 % change for the defined constraints are in the second group. The seventh article limits the variation in C_m.

2.4 Mathematical definition of the optimization problem

In this part, the mathematical definition of the optimization problem is given. Subscripts 1, 2, and 3 are used to define M = 0.08, M = 0.2, and M = 0.35 cases, respectively. Eq. (3) describes $f(x)$.

$$\text{Maximize}\left(\frac{(C_l / C_d)_2}{173.56}\right). \tag{3}$$

The constraints are shown between Eqs. (4) and (18).

$$1-\frac{(C_l)_1}{1.769}\le 0 \tag{4}$$

$$\frac{(C_d)_1}{0.054\cdot 1.1}-1\le 0 \tag{5}$$

$$-1-\frac{(C_m)_1}{0.0369\cdot 1.75}\le 0 \tag{6}$$

$$\frac{(C_m)_1}{0.0369\cdot 0.25}+1\le 0 \tag{7}$$

$$\frac{(C_l)_2}{0.916\cdot 1.1}-1\le 0 \tag{8}$$

$$1-\frac{(C_l)_2}{0.916\cdot 0.9}\le 0 \tag{9}$$

$$-1-\frac{(C_m)_2}{0.0991\cdot 1.75}\le 0 \tag{10}$$

$$\frac{(C_m)_2}{0.0991\cdot 0.25}+1\le 0 \tag{11}$$

$$\frac{(C_d)_3}{0.0054}-1\le 0 \tag{12}$$

$$\frac{(C_l)_3}{0.261\cdot 1.1}-1\le 0 \tag{13}$$

$$1-\frac{(C_l)_3}{0.261\cdot 0.9}\le 0 \tag{14}$$

$$-1-\frac{(C_m)_2}{0.1093\cdot 1.75}\le 0 \tag{15}$$

$$\frac{(C_m)_2}{0.1093\cdot 0.25}+1\le 0 \tag{16}$$

$$\frac{wl}{3.07\cdot 1.1}-1\le 0 \tag{17}$$

$$-\frac{A}{0.184\cdot 0.9}+1\le 0\,. \tag{18}$$

The total number of constraints, which are all inequality constraints, is 15. Eqs. (19)-(24) show the upper and lower bounds of the design variables. α_1, α_2, and α_3 are the design variables corresponding to M = 0.08, M = 0.2, and M = 0.35 cases, respectively.

$$0.25\le\frac{m}{0.08}\le 1 \tag{19}$$

$$0.15\le\frac{p}{0.8}\le 0.75 \tag{20}$$

$$0.5\le\frac{t}{0.16}\le 1 \tag{21}$$

$$0.5\le\frac{\alpha_1}{20}\le 1 \tag{22}$$

$$0\le\frac{\alpha_2}{15}\le 1 \tag{23}$$

$$-1\le\frac{\alpha_3}{6}\le 1\,. \tag{24}$$

As observed, the objective function is scaled using the

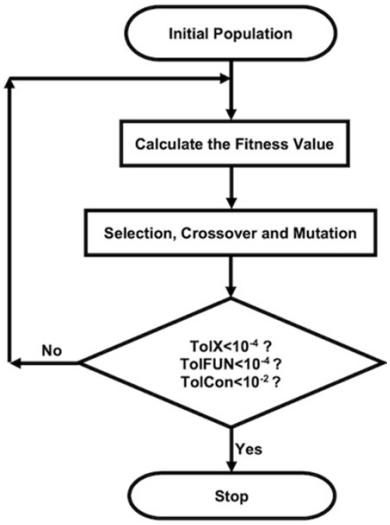

Fig. 1. Flowchart of GA.

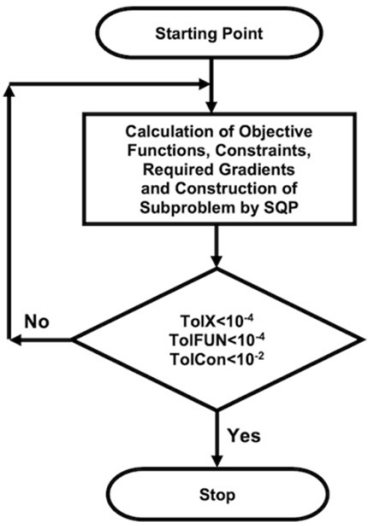

Fig. 2. Flowchart of GA.

$C_l / C_{d\max}$ of NACA 4412. The limits discussed in the scenario and the upper bounds of the design variables are used for the scaling of the constraints and the design variables, respectively.

2.5 Optimization solvers

In this part of the study, the optimization solvers are GA and SQP, and the parameters related to their proper use are discussed.

GA is an evolutionary algorithm based on the natural selection process. The use of the algorithm began after the pioneer study of Holland [22]. The optimization process, as shown in Fig. 1, starts with the definition of initial population. Here, the initial population does not need to be defined. Then, the fitness score of the population individuals is calculated using Xfoil. Thereafter, the fittest individuals are selected, and crossover is performed to generate offspring by swapping parts of the fittest individuals. Mutation is applied to prevent premature convergence to local optimum by randomly sampling new points in the design space.

The selection of GA parameters is based on studies of Williams and Crossley [23] and Saleem and Kim [24]. Each design variable is coded to binary strings of 12 bits, and the total chromosome length (l) becomes 72 because six design variables are considered. According to Eq. (25), the population size (N) is calculated.

$$N = 4l . \tag{25}$$

Mutation rate (MR) is calculated using Eq. (26). The crossover rate is set to 0.5.

$$MR = \frac{l+1}{2Nl} . \tag{26}$$

The termination criteria are defined as 10^{-4} for the change in the design variable array norm (TolX) and for the change in the objective function (TolFUN). The solution is feasible if the maximum constraint violation (TolCon) is less than 0.01. Augmented Lagrangian GA is selected to satisfy the nonlinear constraints [25]. Parallel programming is applied for the analysis by using GA options of MATLAB.

SQP is the most recent method among the gradient-based optimization methods, and its main advantage is to solve the problem by calling the least number of gradient evaluations [26]. As shown in Fig. 2, the starting point is defined first. Then, the objective function, the constraints, and their gradients with respect to design variables are calculated, and the quadratic subproblem for the solution is constructed by SQP. Central difference is applied for the calculation of the gradient of the objective function and the Jacobian matrix of the constraints. Parallel computing is used for these calculations.

2.6 Results

This part discusses the aerodynamic optimization results of NACA four-digit airfoil series. The optimization problem that is defined above is solved for three times. In the first case (C1), the optimum airfoil is obtained by the sequential use of GA and SQP. For this case, NACA 4412 and the α values depicted in Table 2 are defined as the initial population for GA. After GA is performed, the optimum airfoil and α data taken from GA are defined as the initial point for SQP. The second case (C2) is nearly identical to C1 except the definition of initial population. In C2, no initial population is defined in GA. In the third case (C3), the optimum airfoil is obtained using SQP only. For this case, NACA 4412 and the α values depicted in Table 2 are also defined as the initial point.

MATLAB R2022a and Xfoil Version 6.97 are used in the analysis. The results are obtained on a 2.3 GHz Intel Core i9, 32 GB MacBook Pro. The physical cores are used in the parallel programming.

Table 3. Optimization results for C1, C2, and C3.

	f(x)	Max g(x)	G/I	FC	ST (s)
C1-GA	1.187	0.008	3/161	42966	3884
C1-SQP	1.2	0	7	31	29
C2-GA	1.185	0.01	3/391	105756	9362
C2-SQP	1.208	0.009	4	32	32
C3	1.197	0	7	26	23

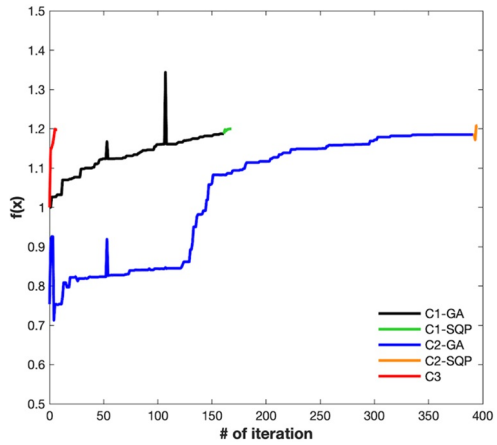

Fig. 3. Variation in f(x) with I.

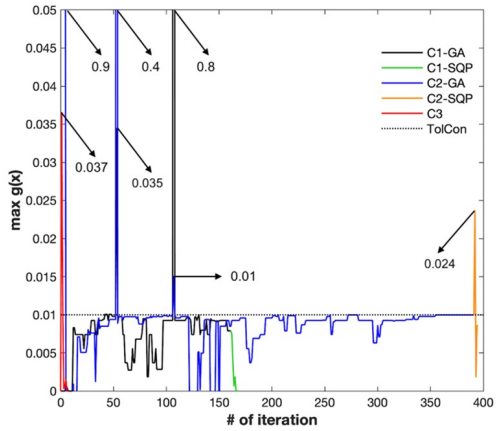

Fig. 4. Variation in max g(x) with I.

The optimization results in terms of $f(x)$, maximum $g(x)$ violation, number of generations (G), iteration number (I), function count (FC), and solution time (ST) are depicted in Table 3.

C2 calculates the highest objective function according to the results. However, the maximum of $g(x)$ is nearly at the limit, which is 0.01. The stand-alone use of SQP captures nearly the same results as obtained by the sequential use of GA and SQP in C1 and C2. In addition, the ST of C3 is significantly shorter than the ST of C1 and C2. When C1 and C2 are compared, defining a feasible initial population decreases ST evidently. Figs. 3 and 4 depict the variation in $f(x)$ and max $g(x)$ with I.

Table 4. Significant aerodynamic results of C1.

	NACA 4412	C1	
		GA	SQP
$(C_l / C_{dmax})_2$	173.56	206.09	208.22
$(C_l)_1 \geq 1.769$	1.769	1.793	1.794
$(C_d)_1 \leq 0.0594$	0.054	0.0577	0.0579
$-0.065 \leq (C_m)_1 \leq -0.009$	−0.0369	−0.0554	−0.0568
$0.828 \leq (C_l)_2 \leq 1.01$	0.916	1.016	1.008
$-0.173 \leq (C_m)_2 \leq -0.024$	−0.0991	−0.1260	−0.1273
$0.235 \leq (C_l)_3 \leq 0.287$	0.261	0.287	0.286
$(C_d)_3 \leq 0.0054$	0.0054	0.0054	0.0054
$-0.191 \leq (C_m)_3 \leq -0.027$	−0.1093	−0.1325	−0.1348
$wl \leq 3.377(m)$	3.071	3.069	3.069
$A \geq 0.165(m^2)$	0.184	0.166	0.165

Table 5. Significant aerodynamic results of C2.

	NACA 4412	C2	
		GA	SQP
$(C_l / C_{dmax})_2$	173.56	205.67	209.63
$(C_l)_1 \geq 1.769$	1.769	1.802	1.802
$(C_d)_1 \leq 0.0594$	0.054	0.048	0.051
$-0.065 \leq (C_m)_1 \leq -0.009$	−0.0369	−0.0598	−0.0589
$0.828 \leq (C_l)_2 \leq 1.01$	0.916	1.018	1.017
$-0.173 \leq (C_m)_2 \leq -0.024$	−0.0991	−0.127	−0.129
$0.235 \leq (C_l)_3 \leq 0.287$	0.261	0.239	0.287
$(C_d)_3 \leq 0.0054$	0.0054	0.0054	0.0054
$-0.191 \leq (C_m)_3 \leq -0.027$	−0.1093	−0.1387	−0.1365
$wl \leq 3.377(m)$	3.071	3.071	3.069
$A \geq 0.165(m^2)$	0.184	0.171	0.165

As shown in Figs. 3 and 4, the GA of C1 has feasible results apart from the jumps at the generation change. The max $g(x)$ values become 0.035 and 0.8 at the first and second generation, respectively. All results of SQP of C1 are feasible. No initial population is defined for the GA of C2. Thus, the solution starts totally in the infeasible region, where max $g(x)$ is around 0.9, but it goes to the feasible region after the fifth iteration. During this change, $f(x)$ increases from 0.75 to 0.92 and then decreases to 0.72. Similar to the GA of C1, that of C2 has infeasible results at the generation change. The SQP of C2 becomes infeasible at first iteration and then returns to the feasible region. C3 is in the infeasible region for the first two iterations and then returns to the feasible region. Max $g(x)$ becomes 0.037 during the solution for this case.

Table 6. Significant aerodynamic results of C3.

	NACA 4412	SQP
$(C_l / C_{dmax})_2$	173.56	207.84
$(C_l)_1 \geq 1.769$	1.769	1.801
$(C_d)_1 \leq 0.0594$	0.054	0.051
$-0.065 \leq (C_m)_1 \leq -0.009$	−0.0369	−0.0577
$0.828 \leq (C_l)_2 \leq 1.01$	0.916	1.01
$-0.173 \leq (C_m)_2 \leq -0.024$	−0.0991	−0.127
$0.235 \leq (C_l)_3 \leq 0.287$	0.261	0.286
$(C_d)_3 \leq 0.0054$	0.0054	0.0054
$-0.191 \leq (C_m)_3 \leq -0.027$	−0.1093	−0.1349
$wl \leq 3.377(m)$	3.071	3.069
$A \geq 0.165(m^2)$	0.184	0.165

Table 7. Optimum design variables of C1, C2, and C3.

	NACA 4412	C1	C2	C3
$0.02 \leq m \leq 0.08$	0.04	0.0491	0.0496	0.0491
$0.12 \leq p \leq 0.6$	0.4	0.402	0.403	0.403
$0.08 \leq t \leq 0.16$	0.12	0.108	0.108	0.108
$10 \leq \alpha_1 \leq 20$	18	17.66	17.08	17.09
$0 \leq \alpha_2 \leq 15$	4	3.73	3.73	3.73
$-6 \leq \alpha_3 \leq 6$	−2	−2.71	−2.76	−2.71

Tables 4 and 6 show the significant aerodynamic results of the optimum airfoils. Among the constraints, $(C_l)_2$, $(C_l)_3$, $(C_d)_3$, and A are satisfied at their limits. For all optimum airfoils, constraint related to $(C_l)_1$ is satisfied with a significant difference from its limit. wl is nearly unaltered. The C_m of the optimum airfoils changes between 20 % and 60 % compared with NACA 4412. Its highest change is observed at high α. The variation in the optimization results is very small when SQP is applied after GA.

Table 7 shows the optimum design variables of C1, C2, and C3. As observed, the optimum design variables are nearly identical to one another. The difference between the second and third decimals of the optimum design variables creates the difference in the optimum $f(x)$ and the corresponding maximum $g(x)$. If the change in the design variables is interpreted, then the t of the optimum airfoils is 10 % less than the t of NACA 4412. This change decreases the drag. m is increased around 24 % by the optimization solvers to increase $(C_l / C_d)_2$ and satisfy the constraint related to C_l. Notably, p is nearly unaltered.

The optimum airfoils are shown in Figs. 5-7. For C1, the change in the airfoil with generations is significant. m increases and t decreases with generations. As discussed above, the $(C_l)_1$ of the optimum airfoils is higher than the $(C_l)_1$ of

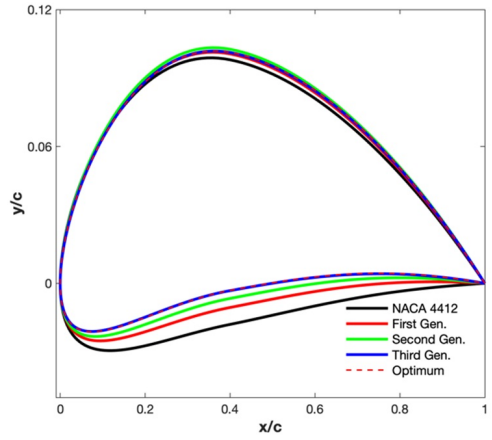

Fig. 5. Optimum airfoils for C1.

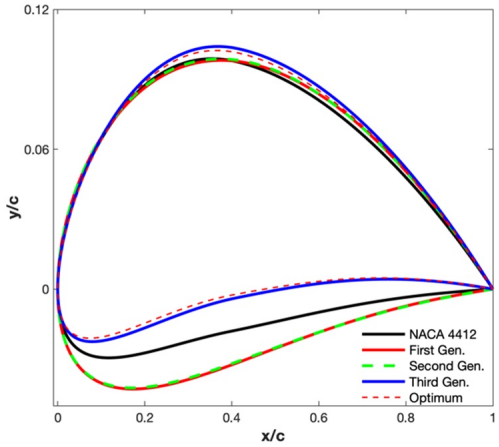

Fig. 6. Optimum airfoils for C2.

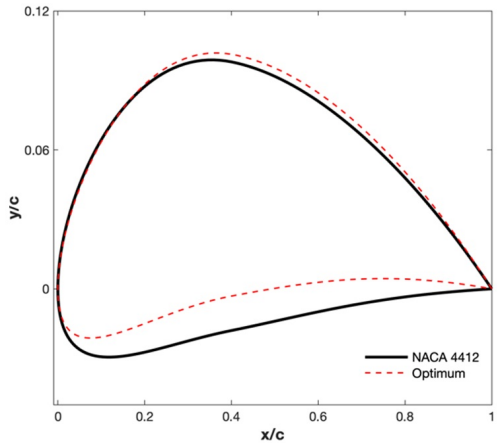

Fig. 7. Optimum airfoils for C3.

NACA 4412. This finding is due to the increment in m. Contrary to the gradual variation observed in C1, the airfoil is thicker, less cambered, and p shifts reward at the first and second generations for C2. However, the optimum airfoil shape shows similar changes discussed for C1 at the third generation. Fig. 7 shows the optimum airfoil for C3.

3. Conclusions

This study proposes the comparison of GA and SQP for NACA four-digit airfoil series optimization. The main findings are listed as follows:

1) The performance of airfoils at different angle of attack values should be defined into the optimization problem as the functional constraints for their practical design.

2) Among the functional constraints, the constraints related to low angle of attack, which is the maximum velocity phase, reach their limit. Therefore, these constraints restrict the further increment in the objective function.

3) The constraint related to the cross-sectional area reaches its limit whereas the wetted area is nearly unaltered according to the results. In other words, the constraint related to the cross-sectional area is the only sufficient geometric constraint.

4) The performance of the system at different conditions, except the condition at which maximization or minimization of the objective function is sought, is defined into the optimization problem as the functional constraints. In this case, SQP nearly converges to the optimum calculated by GA in a remarkably shorter time.

5) An initial population that sets the optimization problem into the feasible region should be defined to decrease the computational cost and solution time for GA.

6) The optimization solvers decrease the maximum thickness ratio to maximize the lift-to-drag ratio, and this decline yields a decrease in drag. The maximum camber is also increased, which improves the lift. The maximum camber location is nearly unaltered.

Nomenclature

a : Speed of sound
$A.$: Cross-sectional area
α : Angle of attack
c : Reference length
C_d : Drag coefficient
C_l : Lift coefficient
C_m : Moment coefficient
$f(x)$: Objective function
FC : Function count
GA : Genetic algorithm
$g(x)$: Constraints
G : Number of generations
I : Number of iterations
l : Total chromosome length
m : Maximum camber
M : Mach number
μ_∞ : Dynamic viscosity
MR : Mutation rate
n : Amplification factor
N : Number of panels
N : Population size
p : Maximum camber location
Re : Reynolds number
ρ_∞ : Density
SQP : Sequential quadratic programming
ST : Solution time
t : Maximum thickness
$TolFUN$: Change in objective function
$TolCon$: Maximum constraint violation
$TolX$: Change in design variable array norm
V_∞ : Free stream velocity
wl : Wetted length
z_c : Camber distribution
z_t : Thickness distribution

References

[1] R. M. Pinkerton, *The Variation with Reynolds Number of Pressure Distribution over an Airfoil Section*, NACA-TR-613, US Gov. (1938).

[2] I. H. Abbott and A. E. Von Doenhoff, *Theory of Wing Sections: Including a Summary of Airfoil Data*, Courier Corporation, Massachusetts (2012).

[3] D. Lednicer, *The Incomplete Guide to Airfoil Usage*, UIUC Applied Aerodynamics Group, https://m-selig.ae.illinois.edu/ads/aircraft.html (2010).

[4] P. Gamboa, J. Vale, F. L. P. Lau and A. Suleman, Optimization of a morphing wing based on coupled aerodynamic and structural constraints, *AIAA Journal*, 47 (9) (2009) 2087-2104.

[5] S. N. Leloudas, G. A. Strofylas and I. K. Nikolos, Constrained airfoil optimization using the area-preserving free-form deformation, *Aircraft Engineering and Aerospace Technology*, 90 (6) (2018) 914-926.

[6] S. Koziel and L. Leifsson, Multi-level cfd-based airfoil shape optimization with automated low-fidelity model selection, *Procedia Computer Science*, 18 (2013) 889-898.

[7] B. K. Woods, J. H. Fincham and M. I. Friswell, Aerodynamic modelling of the fish bone active camber morphing concept, *Proceedings of the RAeS Applied Aerodynamics Conference*, Bristol, UK (2014).

[8] M. V. Pricop, M. Boşcoianu, M. G. Cojocaru and A. Dumitrache, Airfoil optimization based on low fidelity flow models, *AIP Conference Proceedings*, Yerevan, Armenia, 2046 (1) (2018).

[9] M. Drela, XFOIL: an analysis and design system for low Reynolds number airfoils, T. J. Mueller (eds), *Low Reynolds Number Aerodynamics. Lecture Notes in Engineering*, Springer, Berlin, 54 (1989), https://doi.org/10.1007/978-3-642-84010-4_1.

[10] J. F. Herbert-Acero, O. Probst, C. I. Rivera-Solorio, K. K. Castillo-Villar and S. Méndez-Díaz, An extended assessment of fluid flow models for the prediction of two-dimensional steady-state airfoil aerodynamics, *Mathematical Problems in Engineering*, 2015 (2015) 854308.

[11] D. S. Körpe and Ö. Ö. Kanat, Aerodynamic optimization of a UAV wing subject to weight, geometric, root bending moment, and performance constraints, *International Journal of Aerospace Engineering*, 2019 (2019) 3050824.

[12] N. V. Nikolaev, Optimization of airfoils along high-aspect-ratio

wing of long-endurance aircraft in trimmed flight, *Journal of Aerospace Engineering*, 32 (6) (2019) 04019090.
[13] A. Garcia-Gutierrez, J. Gonzalo, D. Dominguez, D. Lopez and A. Escapa, Aerodynamic optimization of propellers for high altitude pseudo-satellites, *Aerospace Science and Technology*, 96 (2020) 105562.
[14] J. Hnidka, D. Rozehnal and K. Maňas, Optimization of SUAV's propeller in a hover, *Proceedings of MATEC Web of Conferences*, Vyhne, Slovak Republic, 313 (2020).
[15] M. Thapa and S. Missoum, Stochastic optimization of a horizontal-axis composite wind turbine blade, *Proceedings of ASME International Mechanical Engineering Congress and Exposition*, Virtual, Online (2020).
[16] H. Muhsen, W. Al-Kouz and W. Khan, Small wind turbine blade design and optimization, *Symmetry*, 12 (1) (2020) 18.
[17] B. H. Dennis, G. S. Dulikravich and Z. X. Han, Constrained shape optimization of airfoil cascades using a Navier-Stokes solver and a genetic/SQP algorithm, *Proceedings of the ASME 1999 International Gas Turbine and Aeroengine Congress and Exhibition. Volume 1: Aircraft Engine; Marine; Turbomachinery; Microturbines and Small Turbomachinery*, Indianapolis (1999).
[18] D. Cinquegrana and E. Iuliano, Investigation of adaptive design variables bounds in dimensionality reduction for aerodynamic shape optimization, *Computers and Fluids*, 174 (2018) 89-109.
[19] M. Li, J. Bai, L. Li, X. Meng, Q. Liu and B. Chen, A gradient-based aero-stealth optimization design method for flying wing aircraft, *Aerospace Science and Technology*, 92 (2019) 156-169.
[20] The Massachusetts Institute of Technology Website, *XFOIL Subsonic Airfoil Development System*, https://web.mit.edu/drela/Public/web/xfoil/xfoil6.99.tgz (Accessed 21 November 2021).
[21] G. Brown, *Xfoil Interface*, MathWorks, https://www.mathworks.com/matlabcentral/fileexchange/30446-xfoil-interface (Accessed 21 November 2021).
[22] J. H. Holland, *Adaption in Natural and Artificial Systems: An Introductory Analysis with Application to Biology, Control and Artificial Intelligence*, University of Michigan Press, Ann Arbor, USA (1975).
[23] E. A. Williams and W. A. Crossley, Empirically-derived population size and mutation rate guidelines for a genetic algorithm with uniform crossover, *Soft Computing in Engineering Design and Manufacturing*, 1st edn., Springer, London, UK (1998) 163-172.
[24] A. Saleem and M. H. Kim, Aerodynamic performance optimization of an airfoil-based airborne wind turbine using genetic algorithm, *Energy*, 203 (2020) 117841.
[25] A. R. Conn, N. Gould and P. L. Toint, A globally convergent augmented lagrangian barrier algorithm for optimization with general inequality constraints and simple bounds, *Mathematics of Computation*, 66 (217) (1997) 261-288.
[26] G. N. Vanderplaats, *Numerical Optimization Techniques for Engineering Design*, Vanderplaats Research and Development. Inc., Colorado Springs, USA (1999).

Durmuş Sinan Körpe received his Ph.D. in Aerospace Engineering from Middle East Technical University. He is an Associate Professor doctor of the Department of Aerospace Engineering, Hasan Kalyoncu University, Gaziantep, Türkiye. His research interests include CFD, low-speed aerodynamics, and optimization.

Ibrahim Halil Güzelbey received his Ph.D. in Mechanical Engineering from Cranfield University. He is a Professor doctor of the Department of Aerospace Engineering, Hasan Kalyoncu University, Gaziantep, Türkiye. His research interests include CFD, optimization, and olid mechanics.